



A protocol for preparing nucleotide-free KaiC monomer

Atsushi Mukaiyama^{1,2,3}, Masato Osako⁴, Takaaki Hikima³, Takao Kondo⁴ and Shuji Akiyama^{1,2,3}

¹Research Center of Integrative Molecular Systems (CIMoS), Institute for Molecular Science, 38 Nishigo-Naka, Myodaiji, Okazaki 444-8585, Japan

²Department of Functional Molecular Science, SOKENDAI (The Graduate University for Advanced Studies), 38 Nishigo-Naka, Myodaiji, Okazaki 444-8585, Japan

³RIKEN SPring-8 Center, Harima Institute, 1-1-1 Kouto, Sayo, Hyogo 679-5148, Japan

⁴Division of Biological Science, Graduate School of Science, Nagoya University, Furo-cho, Chikusa-ku, Nagoya 464-8602, Japan

Received February 20, 2015; accepted March 12, 2015

The hexameric form of the KaiC protein is a core of the cyanobacterial biological clock, and its enzymatic activities exhibit circadian periodicity. The instability of the monomeric form of nucleotide-free KaiC has precluded its storage and detailed analyses of the activities of the reassembled hexamer. Here, we provide a protocol for preparing nucleotide-free KaiC monomer that is stable in solution and for triggering its reassembly into intact KaiC hexamer by the addition of ATP. A phosphate buffer containing glutamic acid and arginine enhanced the stability of KaiC monomer considerably. In addition, we found that reassembled KaiC hexamer was functionally active as the intact hexamer. This protocol provides a methodological basis for further analyses of first-turnover events of the ATPase/autokinase/autophosphatase activities of the KaiC hexamer.

Key words: circadian clock, KaiC, solution structure

KaiC, a core protein of the cyanobacterial circadian clock, self-assembles into a hexameric form upon binding ATP [1]. The KaiC hexamer exhibits rhythmic ATPase/autokinase/autophosphatase activities [2,3] both *in vivo* [4] and *in vitro* [5] in the presence of ATP and two other clock-proteins,

KaiA and KaiB. These rhythms satisfy three characteristics shared among a wide range of circadian clocks: self-sustained circadian oscillation [5], minimal dependence of period on ambient temperature [5] (temperature compensation), and entrainment of the oscillator by external stimuli [6]. The ATPase activity of KaiC, which exhibits a close correlation with the oscillatory frequency [3], is considered to be one of the period-determining factors of the cyanobacterial circadian clock.

Recent studies have indicated that the monomeric form of KaiC is useful in analyses of the properties of the KaiC hexamer. The KaiC monomer consists of an N-terminal C1 domain and a C-terminal C2 domain. Chang *et al.* prepared a monomeric truncate of the C1 domain and proposed that it could interact with KaiB [7]. Nishiwaki *et al.* prepared full-length KaiC monomer in the presence of excess ADP (0.1 mM), and used this molecule to analyze the auto-dephosphorylation kinetics of the KaiC hexamer [8]. However, a major problem concerning the monomeric KaiC has been its instability in the absence of any nucleotides (ATP/ADP). This technical issue has precluded not only storage of nucleotide-free KaiC monomer, but also detailed physicochemical measurements, *e.g.*, pre-steady-state analysis of enzymatic activities upon addition of ATP to nucleotide-free KaiC monomer.

In this paper, we describe an experimental protocol for preparing and storing nucleotide-free KaiC monomer with improved stability. The stable monomeric conformation of KaiC was verified by size-exclusion chromatography (SEC) and small-angle X-ray scattering (SAXS) techniques. The biological intactness of the KaiC monomer was confirmed

Abbreviations: SAXS, small-angle X-ray scattering; SEC, size-exclusion chromatography

Corresponding author: Shuji Akiyama, Research Center of Integrative Molecular Systems (CIMoS), Institute for Molecular Science, 38 Nishigo-Naka, Myodaiji, Okazaki 444-8585, Japan.
e-mail: akiyamas@ims.ac.jp

biochemically by investigating the phosphorylation cycle of the reconstructed KaiC hexamer. This protocol provides a practical means for further biochemical and biophysical analyses of KaiC, which should facilitate a greater understanding of the cyanobacterial circadian clock.

Materials and Methods

Phosphorylation Cycle of Purified KaiC Protein

Recombinant Kai proteins were expressed and purified as previously described [9,10]. Using the purified Kai proteins, the KaiC phosphorylation cycle was reconstructed *in vitro* as previously described [2,5].

Preparation of Nucleotide-free KaiC Monomer

Disassembly of the KaiC hexamer was induced by removing ATP molecules present in a purified fraction containing KaiC hexamer. Unless otherwise stated, this was accomplished by passing the sample through a column (HiPrepDesalting 26/10, GE Healthcare) thoroughly equilibrated with a buffer (P-buffer: 50 mM NaH_2PO_4 , 150 mM NaCl, 5 mM MgCl_2 , 2 mM DTT, pH 7.8) containing 50 mM L-arginine and 50 mM L-glutamic acid. The ATP-depleted fraction was collected and incubated on ice for 24 h, and then subjected to size-exclusion gel chromatography (SEC) (Superdex200, GE Healthcare) to obtain a purified fraction containing nucleotide-free KaiC monomer.

SAXS

SAXS data were taken at RIKEN Structural Biology Beamline I (BL45XU) using either a Pilatus 300K-W detector or a charge-coupled device equipped with an X-ray image intensifier [11], each of which was calibrated against the powder diffraction peak of silver behenate [12]. A series of diluted samples and a matching buffer were introduced into the respective chambers of an octuplet cuvette [13], and then irradiated individually to obtain a data set of the scattering curves, $I(Q)$, where $Q=4\pi\sin\theta/\lambda$, 2θ is the scattering angle and λ is the X-ray wavelength (0.9 or 1.0 Å). After scaling to the X-ray intensity, the exposure time, and the particle concentration, the contribution of the buffer was removed by interchamber subtraction as previously described [13]. The innermost portion of $I(Q)$ was fitted under the Guinier approximation [14] using the following equation:

$$\ln I(Q) = \ln I(0) - \frac{R_g^2}{3} Q^2$$

where $I(0)$ and R_g are the forward scattering intensity and the radius of gyration, respectively. Molecular mass standards for SAXS experiments were prepared as previously reported [15]. Rigid-body modeling, ensemble-optimization modeling, and $P(r)$ determination were conducted by using the software packages BUNCH [16], EOM [17], and GNOM [18], respectively. The theoretical SAXS curve of the crystal structure of hexameric KaiC (2GBL) [19] was calculated

using a software CRY SOL [20], and was fitted to the experimental SAXS curve of the reconstructed KaiC using the Q range from 0.01357 to 0.41293 \AA^{-1} .

In both the rigid-body and ensemble modeling, each protomer of KaiC was treated as rigid C1 (residues from 14 to 250) and C2 bodies (residues from 257 to 500) connected by a flexible linker with flexible N- (residues from 1–13) and C-termini (residues from 501 to 519) (see details in Table 2). The atomic coordinate of the rigid parts were taken from the known X-ray crystal structure of KaiC (2GBL) [19]. During the rigid-body refinements, the flexible linker and two termini were assumed as dummy residues, and the relative arrangement of the two rigid bodies were refined against the experimental data while keeping the protein-like geometry of the dummy residues. In the ensemble modeling, a pool of 10,000 hypothetical rigid-body structures of the KaiC monomer was produced as the rigid-body refinements, from which a plausible ensemble was refined against the experimental SAXS data of the nucleotide free-KaiC monomer shown in Figure 3B. The details of the refinement procedure and refinement statistics are summarized in Table 2.

Reconstruction of KaiC Hexamer

The KaiC hexamerization was induced by mixing a solution containing the nucleotide-free KaiC monomer with a P-buffer containing ATP to a final concentration of 1 mM ATP.

Results

Solution conditions optimized for nucleotide-free KaiC monomer

The KaiC hexamer spontaneously disassembles into the monomeric species in the absence of ATP. Due to the limited stability of the KaiC monomers, however, the protein irreversibly forms a large soluble aggregate in Tris buffer (50 mM Tris/HCl, 150 mM NaCl, 5 mM MgCl_2 , 3 mM DTT, pH 8.0) as determined by SEC (red line in Fig. 1A). Although aggregations could be temporarily reduced by fractionating nucleotide-free KaiC monomer by SEC, a dramatic increase in the radius of gyration (R_g), as determined by SAXS, indicated that the protein reassembled into soluble aggregates even on ice (Fig. 1B). This aggregation not only lowers the yield of the nucleotide-free KaiC monomer, but also hinders quantitative biophysical measurements. We found that the use of the P-buffer (50 mM $\text{NaH}_2\text{PO}_4/\text{NaOH}$, 150 mM NaCl, 5 mM MgCl_2 , 3 mM DTT, pH 7.8) containing 50 mM L-arginine and 50 mM L-glutamic acid dramatically improved the stability of the disassembled species. The presence of phosphate anions slowed disassembly of the KaiC hexamer, but the lower-order species persisted without being trapped in soluble aggregates (blue line in Fig. 1A). Because the R_g value remained nearly constant (Fig. 1C), this improvement enabled us to fractionate the purified KaiC monomer on SEC and store it stably at least for 4 h at 10°C.

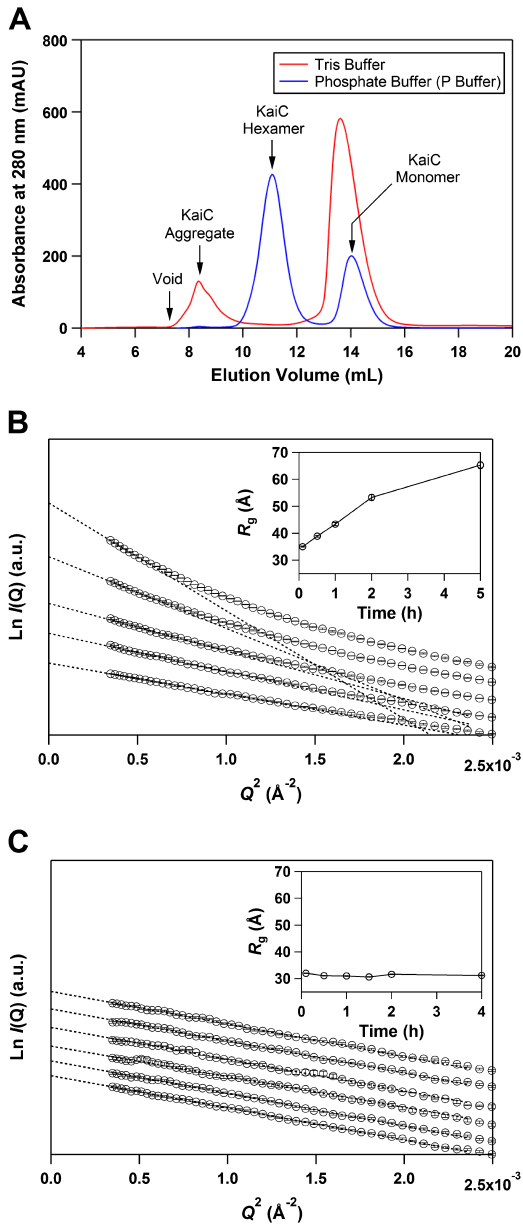


Figure 1 Conditions optimized for nucleotide-free KaiC monomer. (A) Fractionation of nucleotide-free KaiC monomer by size-exclusion chromatography. (B) Irreversible aggregation of nucleotide-free KaiC monomer in a Tris buffer. Fractionated nucleotide-free KaiC monomer (1.53 mg/mL) by SEC was incubated at 10°C, and the aliquots taken from the solution at the indicated time points were used for SAXS measurements. Natural logarithm of X-ray scattering intensity [$\text{Ln}I(Q)$] is plotted against the square of scattering angular momentum (Q^2). Each dotted line shows the linear fit of $\text{Ln}I(Q)$ using the Q range from 0.01866 \AA^{-1} to $Q_{\text{max}} < 1.3/R_g$, whose slope is related to the radius of gyration (R_g) of particles. The plots from bottom to top represent measurements at 0.1, 0.5, 1, 2, and 5 h, all at 10°C. Each plot is longitudinally shifted for clarity of presentation. The inset indicates the time evolution of R_g . (C) Enhanced stability of nucleotide-free KaiC monomer in a P-buffer (50 mM $\text{NaH}_2\text{PO}_4/\text{NaOH}$, 150 mM NaCl, 5 mM MgCl_2 , 3 mM DTT, pH 7.8) containing 50 mM L-arginine and 50 mM L-glutamic acid. Experimental procedure is the same as in Figure 1(B) except for the concentration of KaiC monomer used (0.70 mg/mL). The plots from bottom to top represent the measurements at 0.1, 0.5, 1, 1.5, 2, and 4 h, all at 10°C.

Intactness of nucleotide-free KaiC monomer

Several lines of evidence confirmed the intactness of our preparation of nucleotide-free KaiC monomer. First, we investigated the monomer's size and shape using SAXS (Fig. 2A). Molecular mass estimated from the forward scattering intensity of the KaiC monomer, $I(0)$, was $51.5 \pm 0.6 \text{ kDa}$, consistent with the mass calculated from its amino acid sequence (58.0 kDa) (Table 1). Second, we confirmed that the monomer could undergo reversible hexamerization upon addition of ATP, as validated by the identity of the SAXS curve taken 6 min after addition of ATP to the curve calculated from the X-ray crystal structure of the KaiC hexamer, and also by the 6.05 ± 0.08 -fold increase in $I(0)$ upon addition

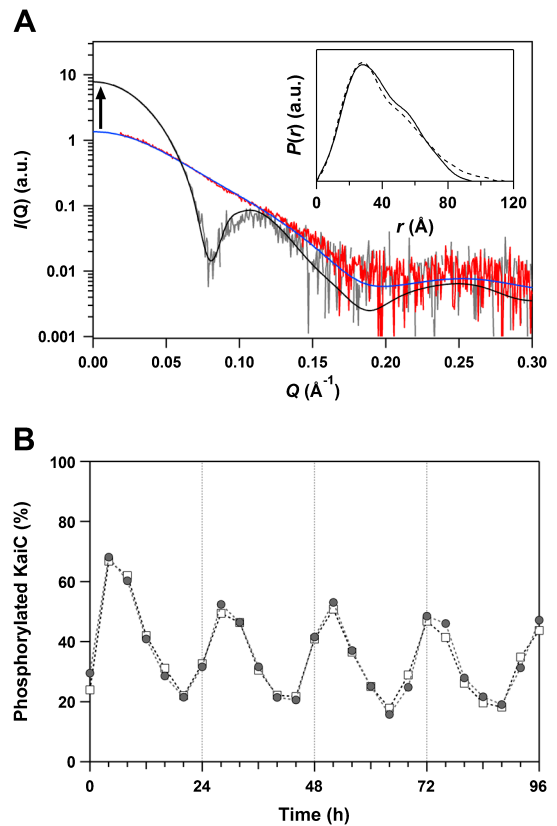


Figure 2 Functional KaiC hexamer reconstructed from intact nucleotide-free KaiC monomer. (A) Comparisons among experimental and theoretical SAXS curves. The red line represents the experimental SAXS curve of the nucleotide-free KaiC monomer at infinite dilution at 10°C. The SAXS curve, displayed as the gray line, was taken at 30°C 6 min after addition of ATP to nucleotide-free KaiC monomer (1.69 mg/ml). Black and blue lines represent the theoretical SAXS curves of the KaiC hexamer ($\chi=3.12$) and one protomer in the KaiC hexamer ($\chi=1.59$), respectively, calculated from the X-ray crystal structure of KaiC [19]. The 6-fold increase in the $I(0)$ value, which is highlighted by the arrow, indicates reversible hexamerization upon the addition of ATP. The inset depicts the experimental pair-distribution function, $P(r)$, for the KaiC monomer (thin line), as well as the theoretical $P(r)$ for the protomer in the KaiC hexamer (dotted line). (B) Comparison between the *in vitro* phosphorylation cycles (at 30°C) of KaiC reconstructed from the nucleotide-free monomer (filled circles) and KaiC never forced to monomerize (open squares).

Table 1 SAXS Structural Parameters

	R_g^a (Å)	R_g^b (Å)	$I(0)^a$ (a.u.)	$I(0)^b$ (a.u.)	D_{max}^c (Å)	V_p^d (Å ³)	MM from $I(0)^e$ (kDa)	MM from V_p^f (kDa)	MM^g (kDa)
Apo KaiC Monomer	30.7±0.4	30.1±0.1	1.37±0.01	1.32±0.01	95	8.9×10^4	51.5±0.6	54	58.0
BSA	28.5±0.3	n.d.	1.77±0.02	n.d.	n.d.	n.d.	n.d.	n.d.	66.4

^aGuinier analysis using the Q range from 0.01847 to $Q_{max} < 1.3/R_g$. ^bEstimates in real space upon $P(r)$ determination. ^cMaximum dimension estimated by using GNOM package. ^dPorod volume estimated from the GNOM output file (Q range from 0.1873 to 0.4127 Å⁻¹) by using ATSAS package [28]. ^eMolecular mass calculated by using the $I(0)$ value for BSA as the standard. ^fMolecular mass calculated according to an empirical relationship ($MM=V_p/1.65$) [28]. ^gTheoretical molecular mass calculated according to amino acid sequences.

Table 2 SAXS shape-reconstruction statistics for apo KaiC monomer

	apo KaiC Monomer
Shape Reconstruction	BUNCH08
Q range (Å ⁻¹)	0.01847–0.41293
Real Space Range (Å)	0–92
Symmetry	P1
Total Number of Residues	519
Total Number of Dummy Residues	38
Dummy Residues	1–13, 251–256, 501–519
Total Number of Known Residues	481
Known Residues Treated as Rigid Bodies	14–250, 257–500
SQRT(χ^2) (mean±S.D.)	2.640–2.712 (2.674±0.023)
Number of Models Reconstructed	10
DAMAVAR NSD (mean±S.D.)	0.964–1.101 (1.041±0.048)
Shape Reconstruction	EOM2.0
Q range (Å ⁻¹)	0.01847–0.41293
Symmetry	P1
Number of Theoretical Curves (Pool Structures)	10000
SQRT(χ^2) (mean±S.D.)	2.393–2.397 (2.396±0.002)
Number of Ensembles Reconstructed	5

of ATP (Fig. 2A). We also confirmed that the re-assembly of the KaiC hexamer completed within 5 min at 30°C. Third and finally, the *in vitro* phosphorylation cycle of KaiC hexamer reconstructed from the nucleotide-free KaiC monomer was virtually indistinguishable from that of KaiC never forced to monomerize (Fig. 2B). In both cases, the ratio of the phosphorylated KaiC was increased and then decreased repeatedly in the circadian fashion with almost identical amplitude, and no phase shifts were observed between them. Together, these observations confirmed the intactness of the nucleotide-free KaiC monomer prepared as described above.

The R_g value (30.7±0.4 Å) for the nucleotide-free KaiC monomer was smaller than that expected for one protomer (32.0 Å) from the X-ray crystal structure of the KaiC hexamer [19]. The pair-distribution function of the nucleotide-free KaiC monomer also suggested that it adopts a more compact conformation than the protomer in the KaiC hexamer (Fig. 3A). These discrepancies are not surprising, because the protomer of KaiC is expected to be flexible and to undergo structural changes upon monomerization. In fact, a rigid-body model refined against the experimental SAXS

curve predicts a compact conformation for the KaiC monomer (Figs. 3A and B, Table 2). Ensemble modeling of the KaiC monomer resulted in minor improvement of the fitting quality (χ from 2.68 to 2.39 in Fig. 3B, Table 2), suggesting that the compact conformation with a shorter C1–C2 inter-domain distance predominates in solution (Fig. 3C). Despite the structural changes and flexibility, the SAXS data confirmed that nucleotide-free KaiC prepared according to our protocol is purely monomeric.

Discussion

The molecular mass of the aggregated KaiC monomer could be roughly estimated from its SEC elution volume to be in the range of 0.7–2 MDa (Fig. 1A). Because this aggregate never disassembled, even after the addition of ATP, the nucleotide-binding sites in the aggregate must be totally blocked due to non-native self-associations of the monomeric species. Therefore, it is important to prevent the lower-order species of KaiC from being trapped in the soluble aggregate.

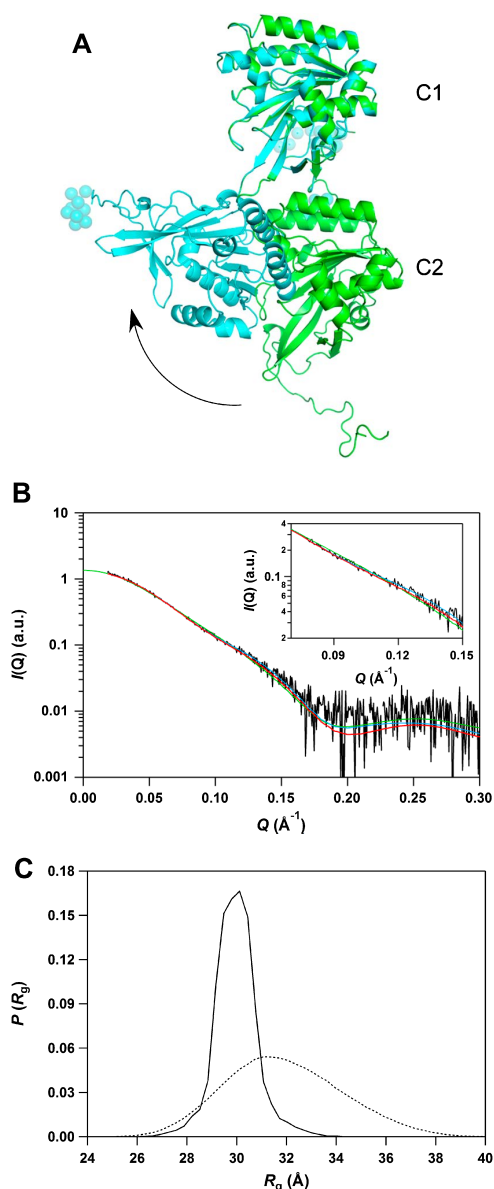


Figure 3 Modeling of nucleotide-free KaiC monomer in solution using the X-ray crystal structure of KaiC hexamer. (A) Possible rigid-body model for the KaiC monomer in solution. The optimum arrangement of the C1 and C2 domains in the KaiC monomer was refined against the experimental SAXS curve of the KaiC monomer (Fig. 2A). The refined model (cyan) is superimposed on the structure of one protomer from the hexamer structure (green), using the C1 domains. Each “blue sphere” represents an approximate $C\alpha$ position of residues treated as “dummy residues” in the BUNCH refinement (see details in Table 2). (B) Experimental SAXS curve of the KaiC monomer (black) compared to theoretical SAXS curves of the rigid-body model (cyan, $\chi=2.68$, most representative model), ensemble-optimized models (red, $\chi=2.39$, representative model), and the protomer contained in the hexamer structure (green, $\chi=3.12$). The inset represents the expanded view for Q in the range from 0.07 to 0.15 \AA^{-1} . (C) Representative result of ensemble-optimized modeling of nucleotide-free KaiC monomer. By using the EOM package [17], we first produced a pool of 10,000 hypothetical structures of the KaiC monomer (dotted line), from which plausible ensembles (thin line) was constructed by refining their size and composition against the experimental SAXS data of the nucleotide free-KaiC monomer shown in Figure 3B. The plots are the average of five independent optimizations.

The lifetime of nucleotide-free KaiC monomer was extended by inclusion of 50 mM phosphate, 50 mM L-glutamic acid, and 50 mM L-arginine in the buffer (Fig. 1C). Although phosphate stabilizes the native structure of proteins in accordance with the Hofmeister series at high concentration, the effect is not significant at concentrations below 50 mM [21]. Instead, phosphate may bind to the KaiC monomer and prevent non-native self-association [22]. Glutamic acid also stabilizes proteins [23], whereas arginine enhances the solubility of proteins and is thus often used to recover recombinant proteins from aggregates [24]. Furthermore, Golovanov *et al.* demonstrated that the presence of 50 mM glutamic acid and 50 mM arginine increased protein solubility [25]. Therefore, under these conditions, it is likely that these three factors have contributed synergistically to prevent trapping of nucleotide-free KaiC monomer into soluble aggregates. Non-native self-association sites might be sequestered by adopting the compact nucleotide-free monomeric form (Fig. 3A), in which the C1–C2 inter-domain distance is shorter (Fig. 3B). A similar stabilizing effect is also anticipated in cells, in which various sugars and polyols stabilize the native structures of proteins.

The ensemble modeling of the KaiC monomer gave rise to the slight improvement of the quality of fitting to the experimental SAXS data (χ from 2.68 to 2.39). However, the resulted χ value was still larger than unity, indicating that the structure of KaiC monomer in solution can be explained strictly neither by the sole rigid-body model (Fig. 3A) nor their ensemble model (Fig. 3C). This discrepancy may come from a partial deformation of the C2 domain in the KaiC monomer, because a truncated construct of KaiC without the C1 domain cannot form a hexameric ring as stable as that without the C2 domain [26].

Conclusion

In this study, we established a protocol for preparing nucleotide-free KaiC monomer and triggering its reassembly into intact KaiC hexamer by adding ATP. This protocol should be useful for not only building stable mosaic hexamers of KaiC [27], but also characterizing first-turnover events of the ATPase [3]/autokinase [2]/autophosphatase [2] activities of the KaiC hexamer, each of which is crucial for the temperature-compensated circadian periodicity of the Kai-protein clock system. Our protocol offers an ideal means for performing pre-steady-state analyses of KaiC in the absence of ADP, which may competitively inhibit ATP binding. Thus, this method should facilitate a greater understanding of the unique properties of the KaiC protein.

Acknowledgment

The synchrotron radiation experiments were performed on beamline BL45XU at the SPring-8 facility with the approval of RIKEN (proposal No. 20130097, 20140068). This work

was supported by Grants-in-Aid for Scientific Research (to SA, KT, and AM) and partly by nanotechnology Platform Program (Molecule and Material Synthesis) from the Ministry of Education, Culture, Sports, Science and Technology (MEXT) of Japan.

Conflict of Interest

All the authors declare that they have no conflict of interest.

Author Contribution

AM and SA designed the experiments. AM, MO, TH and SA performed the experiments. AM, MO and SA analyzed the data. AM, TK and SA wrote the paper.

References

- [1] Hayashi, F., Suzuki, H., Iwase, R., Uzumaki, T., Miyake, A., Shen, J. R., *et al.* ATP-induced hexameric ring structure of the cyanobacterial circadian clock protein KaiC. *Genes Cells* **8**, 287–296 (2003).
- [2] Nishiwaki, T., Satomi, Y., Kitayama, Y., Terauchi, K., Kiyohara, R., Takao, T., *et al.* A sequential program of dual phosphorylation of KaiC as a basis for circadian rhythm in cyanobacteria. *EMBO J.* **26**, 4029–4037 (2007).
- [3] Terauchi, K., Kitayama, Y., Nishiwaki, T., Miwa, K., Murayama, Y., Oyama, T., *et al.* ATPase activity of KaiC determines the basic timing for circadian clock of cyanobacteria. *Proc. Natl. Acad. Sci. USA* **104**, 16377–16381 (2007).
- [4] Tomita, J., Nakajima, M., Kondo, T. & Iwasaki, H. No transcription-translation feedback in circadian rhythm of KaiC phosphorylation. *Science* **307**, 251–254 (2005).
- [5] Nakajima, M., Imai, K., Ito, H., Nishiwaki, T., Murayama, Y., Iwasaki, H., *et al.* Reconstitution of circadian oscillation of cyanobacterial KaiC phosphorylation in vitro. *Science* **308**, 414–415 (2005).
- [6] Yoshida, T., Murayama, Y., Ito, H., Kageyama, H. & Kondo, T. Nonparametric entrainment of the in vitro circadian phosphorylation rhythm of cyanobacterial KaiC by temperature cycle. *Proc. Natl. Acad. Sci. USA* **106**, 1648–1653 (2009).
- [7] Chang, Y. G., Tseng, R., Kuo, N. W. & LiWang, A. Rhythmic ring-ring stacking drives the circadian oscillator clockwise. *Proc. Natl. Acad. Sci. USA* **109**, 16847–16851 (2012).
- [8] Nishiwaki, T. & Kondo, T. Circadian autodephosphorylation of cyanobacterial clock protein KaiC occurs via formation of ATP as intermediate. *J. Biol. Chem.* **287**, 18030–18035 (2012).
- [9] Nishiwaki, T., Satomi, Y., Nakajima, M., Lee, C., Kiyohara, R., Kageyama, H., *et al.* Role of KaiC phosphorylation in the circadian clock system of *Synechococcus elongatus* PCC 7942. *Proc. Natl. Acad. Sci. USA* **101**, 13927–13932 (2004).
- [10] Akiyama, S., Nohara, A., Ito, K. & Maéda, Y. Assembly and disassembly dynamics of the cyanobacterial periodosome. *Mol. Cell* **29**, 703–716 (2008).
- [11] Ito, K., Kamikubo, H., Yagi, N. & Amemiya, Y. Correction method and software for image distortion and nonuniform response in charge-coupled device-based X-ray detectors utilizing X-ray image intensifier. *Jpn. J. Appl. Phys. I* **44**, 8684–8691 (2005).
- [12] Huang, T. C., Toraya, H., Blanton, T. N. & Wu, Y. X-ray-powder diffraction analysis of silver behenate, a possible low-angle diffraction standard. *J. Appl. Cryst.* **26**, 180–184 (1993).
- [13] Akiyama, S. & Hikima, T. Octuple cuvette for small-angle X-ray solution scattering. *J. Appl. Cryst.* **44**, 1294–1296 (2011).
- [14] Andre, G. & Gerard, F. *Small-Angle Scattering of X-rays* (John Wiley & Sons, Inc., New York, 1955).
- [15] Akiyama, S. Quality control of protein standards for molecular mass determinations by small-angle X-ray scattering. *J. Appl. Cryst.* **43**, 237–243 (2010).
- [16] Petoukhov, M. V. & Svergun, D. I. Global rigid body modeling of macromolecular complexes against small-angle scattering data. *Biophys. J.* **89**, 1237–1250 (2005).
- [17] Bernado, P., Mylonas, E., Petoukhov, M. V., Blackledge, M. & Svergun, D. I. Structural characterization of flexible proteins using small-angle X-ray scattering. *J. Am. Chem. Soc.* **129**, 5656–5664 (2007).
- [18] Svergun, D. I. Determination of the regularization parameter in indirect-transform methods using perceptual criteria. *J. Appl. Cryst.* **25**, 495–503 (1992).
- [19] Pattanayek, R., Wang, J., Mori, T., Xu, Y., Johnson, C. H. & Egli, M. Visualizing a circadian clock protein: crystal structure of KaiC and functional insights. *Mol. Cell* **15**, 375–388 (2004).
- [20] Svergun, D. I., Barberato, C. & Koch, M. H. J. CRYSOLO—a program to evaluate X-ray solution scattering of biological macromolecules from atomic coordinates. *J. Appl. Cryst.* **28**, 768–773 (1995).
- [21] Bye, J. W. & Falconer, R. J. Thermal stability of lysozyme as a function of ion concentration: a reappraisal of the relationship between the Hofmeister series and protein stability. *Protein Sci.* **22**, 1563–1570 (2013).
- [22] Wlodawer, A., Walter, J., Huber, R. & Sjolín, L. Structure of bovine pancreatic trypsin inhibitor. Results of joint neutron and X-ray refinement of crystal form II. *J. Mol. Biol.* **180**, 301–329 (1984).
- [23] Arakawa, T. & Timasheff, S. N. The mechanism of action of Na glutamate, lysine HCl, and piperazine-N,N'-bis(2-ethanesulfonic acid) in the stabilization of tubulin and microtubule formation. *J. Biol. Chem.* **259**, 4979–4986 (1984).
- [24] Tsumoto, K., Umetsu, M., Kumagai, I., Ejima, D. & Arakawa, T. Solubilization of active green fluorescent protein from insoluble particles by guanidine and arginine. *Biochem. Biophys. Res. Commun.* **312**, 1383–1386 (2003).
- [25] Golovanov, A. P., Hautbergue, G. M., Wilson, S. A. & Lian, L. Y. A simple method for improving protein solubility and long-term stability. *J. Am. Chem. Soc.* **126**, 8933–8939 (2004).
- [26] Chang, Y. G., Kuo, N. W., Tseng, R. & LiWang, A. Flexibility of the C-terminal, or CII, ring of KaiC governs the rhythm of the circadian clock of cyanobacteria. *Proc. Natl. Acad. Sci. USA* **108**, 14431–14436 (2011).
- [27] Kitayama, Y., Nishiwaki-Ohkawa, T., Sugisawa, Y. & Kondo, T. KaiC intersubunit communication facilitates robustness of circadian rhythms in cyanobacteria. *Nat. Commun.* **4**, 2897 (2013).
- [28] Petoukhov, M. V., Franke, D., Shkumatov, A. V., Tria, G., Kikhney, A. G., Gajda, M. *et al.* New developments in the ATSAS program package for small-angle scattering data analysis. *J. Appl. Cryst.* **45**, 342–350 (2012).